DIMACS Technical Report 2000-43
December 2000

Quantum Walk on the Line

by

Ashwin Nayak [1]
DIMACS Center
Rutgers University
P.O. Box 1179
Piscataway, NJ 08855
`nayak@dimacs.rutgers.edu`

Ashvin Vishwanath [2]
Joseph Henry Laboratories
Department of Physics
Princeton University
Princeton, NJ 08544
`ashvinv@princeton.edu`

[1]Supported by a joint DIMACS-AT&T Post-Doctoral Fellowship and NSF grants STC 91-19999, CCR 99-06105 and EIA 00-80234.
[2]Supported by a C.E. Procter Fellowship.

DIMACS is a cooperative project of Rutgers University, Princeton University, AT&T Bell Laboratories and Bellcore.

DIMACS is an NSF Science and Technology Center, funded under contract STC–91–19999; and also receives support from the New Jersey Commission on Science and Technology.

ABSTRACT

Motivated by the immense success of random walk and Markov chain methods in the design of classical algorithms, we consider *quantum* walks on graphs. We analyse in detail the behaviour of unbiased quantum walk on the line, with the example of a typical walk, the "Hadamard walk". In particular, we show that after t time steps, the probability distribution on the line induced by the Hadamard walk is almost uniformly distributed over the interval $[-t/\sqrt{2},\ t/\sqrt{2}]$. This implies that the same walk defined on the circle mixes in *linear* time. This is in direct contrast with the quadratic mixing time for the corresponding classical walk. We conclude by indicating how our techniques may be applied to more general graphs.

1 Introduction

Random walks on graphs have found many applications in computer science, including randomised algorithms for 2-Satisfiability, Graph Connectivity and probability amplification (see, e.g., [14]). Recently, Schöning [19] discovered a random walk based algorithm similar to that of Papadimitriou [17] that gives an elegant (and the most efficient known) solution to 3-Satisfiability. In general, Markov chain simulation has emerged as a powerful algorithmic tool and has had a profound impact on random sampling and approximate counting [10]. Notable among its numerous applications are estimating the volume of convex bodies [6][1] and approximating the permanent [9]. A few months ago, Jerrum, Sinclair and Vigoda [11] used this approach to solve the long standing open problem of approximating the permanent for general non-negative matrices.

In the spirit of developing similar techniques for quantum algorithms, we consider *quantum* walk on graphs. To date, few general techniques are known for developing and analysing quantum algorithms: *Fourier sampling*, which is typified by the seminal work of Simon [21] and Shor [20], and *amplitude amplification*, which originated in the seminal work of Grover [8]. Barring applications of these techniques, the search for new quantum algorithms has primarily been *ad hoc*. We believe that studying quantum walk on graphs is a step towards providing a systematic way of speeding up classical algorithms based on random walk.

We begin by considering quantum walks in one dimension. Recall that a classical particle doing a random walk on the integer lattice chooses, at every time step, a random direction ("left" or "right") to move in, and moves to the site adjacent to it in that direction. In direct analogy, one may naïvely try to define quantum walk on the line as follows: at every time step, the particle moves, *in superposition*, both left *and* right with equal amplitudes (perhaps with a relative phase difference). However, such a walk is physically impossible, since the global process is non-unitary. It is also easy to verify that the only possible homogeneous (i.e., translationally invariant) unitary processes on the line involving transitions between adjacent lattice sites are the left and right shift operators (up to an overall phase) [13]. This corresponds to the rather uninteresting motion in a single direction. As explained below (and also shown by [13]), it is still possible to construct a unitary walk if the particle has an extra degree of freedom that assists in its motion.

Consider a quantum particle that moves freely on the integer points on the line, and has an additional degree of freedom, its *chirality*, which takes values "left" and "right". A walk on the line by such a particle may be described as follows. At every time step, its chirality undergoes a rotation (a unitary transformation in general) and then the particle moves according to its final chirality state. Figure 1 depicts this two-stage move in a quantum walk where the chirality undergoes a Hadamard transformation. We call this particular walk the "Hadamard walk".

In this paper, we analyse in detail the dynamics of the Hadamard walk on the line. We derive the asymptotic form of the probability induced on the line by observing the position of a particle doing the walk and show that after t time steps, the distribution is almost uniformly distributed over the interval $[-t/\sqrt{2},\ t/\sqrt{2}]$. This implies that the analogously defined walk on the circle *mixes* in *linear* time. This is in immediate contrast with the classical random walk, which mixes in *quadratic* time.[2]

[1]See [12] for the latest progress on this problem.

[2]In this paper, by the δ-*mixing time* of a walk we mean the *first* time (independent of the initial position) at which

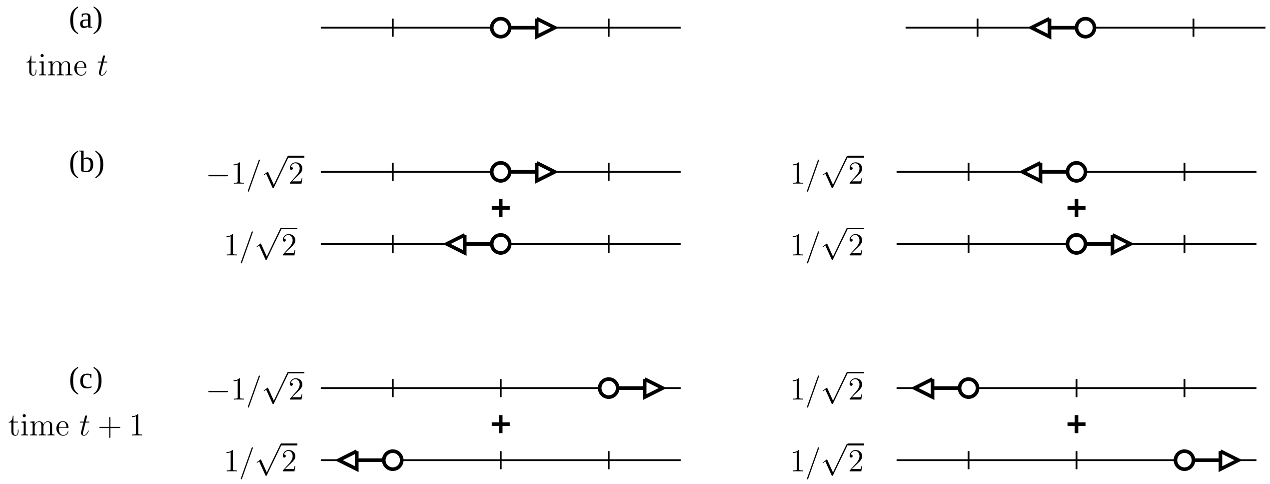

Figure 1: *The dynamics of the Hadamard walk. In (a) we begin at time t with a particle in chirality state "right" or "left". The result of the Hadamard transformation is shown in (b), the particle is now in an equal superposition of "left" and "right" chirality states (with the amplitudes indicated) and then moves accordingly (c) to generate the state at time $t+1$.*

Next, we turn to general quantum walk on the line. Such a walk may involve arbitrary transitions between adjacent lattice points on the line (subject to the global unitarity constraint). It turns out that any homogeneous, local unitary process on the line governing the motion of a particle may be recast as a unitary transformation of the chirality followed by a left/right shift [16]. Moreover, if we are interested in *unbiased* walk[3], we may assume that the particle moves one step to the left if it ends up with chirality "left", and one step to the right if it ends up with chirality "right". Thus, there is no loss in generality in studying only such walk.

It can be shown [16] that if we are interested only in the probability distribution induced on the line by such a walk, we may restrict ourselves to the study of a family of walks specified by a *single* parameter $\theta \in [0, \pi]$. We show that *every* walk in this family, except that for $\theta = 0, \pi$, shares the gross features of the Hadamard walk. In particular, all except the two singular walks mix in linear time.

One method for analysing quantum processes such as the walk we study is the *path integral* approach. This method involves explicitly computing the amplitude of being in a certain state as the sum, over all possible paths leading to that state, of the amplitude of taking that path. The problem of evaluating, or even approximating, path integrals to determine the time development of a wave function is well known to be notoriously hard. We circumvent this barrier by taking the *Schödinger approach*, which takes advantage of the time and space homogeneity of the quantum walk. The

the distribution induced by the walk is δ-close to uniform in total variation distance. The parameter δ is understood to be a constant less than 1 if it is not explicitly specified.

[3] Appendix D has a formal definition of this notion. Essentially, it means that the walk makes no distinction between the two halves of the line given by its initial position. It is not hard to see that in any other kind of (*biased*) unitary walk, the particle moves in a single direction with probability 1 at every time step.

crucial observation is that because of its translational invariance, the walk has a simple description in Fourier space. The Fourier transform of the wave function is thus easily analysed, and transformed back to the spatial domain. It is noteworthy that this technique is standard in the analysis of classical random walk [5].

A key advantage of the Schödinger approach is that the resulting description of the wave function, in terms of integrals of the Fourier type, is amenable to analysis in standard ways. There is a well-developed theory of the asymptotic expansion of integrals [3] which allows us to determine the leading behaviour of the wave function in the large time limit. (This is exactly the case of interest in the design of asymptotically efficient algorithms.) We are thus able to derive the asymptotic functional form of the corresponding probability distribution.

We also use the theory of asymptotic expansion of integrals in a non-standard way to deduce some properties of the probability distribution induced by the walk. For example, we use this method to approximate the probability mass of each point on the line by an integral of the Fourier type. This allows us to calculate the net probability of an interval, and the different moments of the distribution very precisely.

Finally, we note that the asymptotic quantities we calculate match very well with simulation results even for small times, indicating that our results may apply to small quantum systems as well.

Related work

Quantum dynamics similar to ours has previously been studied by Meyer [13] in the context of quantum cellular automata. He singles out the one parameter family of unitary processes mentioned above and derives a closed form solution for the corresponding wave functions. The solution is obtained by following the path integral approach and this allows him to express it in terms of the Gauss hypergeometric function. His motivation in studying such dynamics is however very different from ours, and he does not quantitatively analyse the wave functions further.

In work more closely related to ours in its motivation, Nayak, Schulman and Vazirani [15] have studied random sampling on a quantum computer. They gave an efficient method for generating superpositions for which the corresponding probability distributions satisfy certain well-behavedness properties. Using this for a distribution related by a Fourier transform, they gave an efficient quantum algorithm for sampling from the Gibbs distribution for the Ising model. (Subsequently, Randall and Wilson [18] discovered a *classical* polynomial-time algorithm for this task via a different route.)

Watrous [22] has considered unitary processes based on quantum walk on regular graphs in the context of Undirected Graph Connectivity and logarithmic-space computation. He shows that it is possible to construct, in logarithmic space with limited measurement, and with high probability, a good approximation to the superposition over all vertices connected to a specified vertex in the graph, using a local unitary transform as a subroutine.

We have recently learnt that Aharonov, Ambainis, Kempe and Vazirani [1] have independently studied quantum walks on graphs and their mixing behaviour. They observe that the probability distribution induced by a unitary process on a finite dimensional Hilbert space is essentially periodic and hence does not converge to a stationary distribution. They argue that the notion of mixing in this case is therefore more appropriately captured by the closeness to the uniform distribution, of the *average* of the probability distribution over all time steps. They show that the quantum walk on the n-circle mixes in time $O(n \log n)$ in this sense. They also show a lower bound of $1/d\Phi$ for this mixing time for general graphs, where d is the maximum degree of a vertex in the graph and Φ is its *conductance*.

We have also learnt that Ambainis, Bach and Watrous [2] have analysed the Hadamard walk on the unbounded line, and show that it has linear mixing characteristics. They follow the approach of Meyer, and further analyse the path integrals so obtained to arrive at the result.

Organisation of the paper

The rest of the paper is organised as follows. We formally define and analyse quantum walk on the line in Section 2. Some background on Fourier transforms required for this is summarised in Appendix A. Details of some calculations required for the section are provided in Appendix B. We then consider the behaviour of the walk after large times and derive its asymptotic properties in Section 3. This section is heavily based on the Method of Stationary Phase described in Appendix A. The approximations made in the section are justified in Appendix C. The technique involved in the analysis of the general quantum walk is the same as that for the Hadamard walk. Appendix D summarises the main conclusions about the general case.

2 One dimensional quantum walk

2.1 Formal description of the walk

A particle doing a (classical) symmetric random walk on the line may be described as follows. It starts, say, at the origin, and at every time step, tosses a fair coin. Each of the two possible outcomes of the toss is associated with a distinct direction, "left" or "right". The particle moves one step in the direction resulting from the toss.

A quantum generalisation of this process involves a quantum particle on the line, but with an additional degree of freedom which we call the "chirality". The chirality takes values "left" and "right", and directs the motion of the particle. At any given time the particle may be in a superposition of "left" and "right" chirality states and is therefore described by a two-component wave function. The dynamics of the walk that we consider is given by the following rules. At each time step, the chirality undergoes a rotation (a unitary transformation, in general), and the particle moves according to its final chirality state. Therefore, if the particle ends up with chirality "left", it moves one step to the left, and if it ends up with chirality "right", it moves one step to the right.

For concreteness, we begin by focusing on a quantum walk in which the unitary transformation acting on the chirality state at each time step, is chosen to be the Hadamard transformation (the

Fourier transform over $\mathcal{Z}_2$):

$$\begin{aligned} |\mathrm{L}\rangle &\mapsto \frac{1}{\sqrt{2}}(|\mathrm{L}\rangle + |\mathrm{R}\rangle) \\ |\mathrm{R}\rangle &\mapsto \frac{1}{\sqrt{2}}(|\mathrm{L}\rangle - |\mathrm{R}\rangle). \end{aligned}$$

Here L and R refer to the "left" and "right" chirality states. The resulting quantum walk, which we refer to as the "Hadamard walk" is depicted in Figure 1.

To study the properties of the walk defined above, we consider the wave function describing the position of the particle and analyse how it evolves with time. Let $\Psi(n,t) = \begin{pmatrix} \psi_{\mathrm{L}}(n,t) \\ \psi_{\mathrm{R}}(n,t) \end{pmatrix}$ be the two component vector of amplitudes of the particle being at point n at time t, with the chirality being "left" (upper component) or "right" (lower component). The dynamics for Ψ is then given by the following transformation (cf. Figure 1):

$$\begin{aligned} \Psi(n,t+1) &= \begin{bmatrix} 0 & 0 \\ \frac{1}{\sqrt{2}} & \frac{-1}{\sqrt{2}} \end{bmatrix} \Psi(n-1,t) + \begin{bmatrix} \frac{1}{\sqrt{2}} & \frac{1}{\sqrt{2}} \\ 0 & 0 \end{bmatrix} \Psi(n+1,t) \\ &= M_+\Psi(n-1,t) + M_-\Psi(n+1,t), \end{aligned}$$

for matrices M_+, M_- defined appropriately. Note that this transformation is *unitary* on the basis states given by $\mathcal{Z} \times \mathcal{Z}_2$, since it is the composition of a unitary operation and a reversible move to the left or the right. Moreover, since the particle starts at the origin with chirality state "left" (say), we have the initial conditions, $\Psi(0,0) = \begin{pmatrix} 1 \\ 0 \end{pmatrix}$, and $\Psi(n,0) = \begin{pmatrix} 0 \\ 0 \end{pmatrix}$ if $n \neq 0$.

With the above formulation, the analysis of the Hadamard walk reduces to solving a two dimensional linear recurrence (or a *difference equation*). We show how this recurrence may be analysed in the next section.

2.2 Fourier analysis of the Hadamard walk

As mentioned in Section 1, quantum walk of the kind defined above has, due to translational invariance, a very simple description in the Fourier domain. We therefore cast the problem of time evolution in this basis, where it can easily be solved, and at the end revert back to the real space description by inverting the Fourier transformation. The details are described below.

The spatial Fourier transform $\tilde{\Psi}(k,t)$ (for $k \in [-\pi,\pi]$) of the wave function $\Psi(n,t)$ over $\mathcal{Z}$ is given by (cf. Appendix A)

$$\tilde{\Psi}(k,t) = \sum_n \Psi(n,t)\, \mathrm{e}^{ikn}.$$

In particular, we have $\tilde{\Psi}(k,0) = \begin{pmatrix} 1 \\ 0 \end{pmatrix}$ for all k, for a particle starting at the origin with initially "left" chirality.

From the dynamics of Ψ, we may deduce the following about $\tilde{\Psi}$:

$$\begin{aligned}\tilde{\Psi}(k,t+1) &= \sum_n (M_+\Psi(n-1,t) + M_-\Psi(n+1,t))\, \mathrm{e}^{\mathrm{i}kn} \\ &= \mathrm{e}^{\mathrm{i}k} M_+ \sum_n \Psi(n-1,t)\, \mathrm{e}^{\mathrm{i}k(n-1)} \;+\; \mathrm{e}^{-\mathrm{i}k} M_- \sum_n \Psi(n+1,t)\, \mathrm{e}^{\mathrm{i}k(n+1)} \\ &= \left(\mathrm{e}^{\mathrm{i}k} M_+ + \mathrm{e}^{-\mathrm{i}k} M_-\right) \tilde{\Psi}(k,t).\end{aligned}$$

Thus, we have,

$$\tilde{\Psi}(k,t+1) = M_k\, \tilde{\Psi}(k,t) \tag{1}$$

where

$$M_k = \mathrm{e}^{\mathrm{i}k} M_+ + \mathrm{e}^{-\mathrm{i}k} M_- \tag{2}$$

$$= \frac{1}{\sqrt{2}} \begin{bmatrix} \mathrm{e}^{-\mathrm{i}k} & \mathrm{e}^{-\mathrm{i}k} \\ \mathrm{e}^{\mathrm{i}k} & -\mathrm{e}^{\mathrm{i}k} \end{bmatrix}. \tag{3}$$

Note that $M_k = \Lambda_k U^T$, where Λ_k is the diagonal matrix with entries $\mathrm{e}^{-\mathrm{i}k}, \mathrm{e}^{\mathrm{i}k}$ and U^T is the transpose of the unitary matrix U that acts on the chirality state of the particle. Hence M_k is a unitary matrix. (This general presentation anticipates the walk with general U discussed in Appendix D.)

The recurrence in Fourier space thus takes the simple form $\tilde{\Psi}(k,t+1) = M_k\, \tilde{\Psi}(k,t)$, leading to $\tilde{\Psi}(k,t) = M_k^t\, \tilde{\Psi}(k,0)$. We may calculate M_k^t (and thus $\tilde{\Psi}(k,t)$) by diagonalising the matrix M_k, which is readily done since it is a 2×2 unitary matrix. If M_k has eigenvectors $(|\Phi_k^1\rangle, |\Phi_k^2\rangle)$ and corresponding eigenvalues $(\lambda_k^1, \lambda_k^2)$, we can write:

$$M_k = \lambda_k^1\; |\Phi_k^1\rangle\langle\Phi_k^1| \;+\; \lambda_k^2\; |\Phi_k^2\rangle\langle\Phi_k^2|,$$

and then immediately we obtain the time evolution matrix as:

$$M_k^t \;=\; (\lambda_k^1)^t\; |\Phi_k^1\rangle\langle\Phi_k^1| \;+\; (\lambda_k^2)^t\; |\Phi_k^2\rangle\langle\Phi_k^2|.$$

The eigenvalues of M_k are $\lambda_k^1 = \mathrm{e}^{-\mathrm{i}\omega_k}$ and $\lambda_k^2 = \mathrm{e}^{\mathrm{i}(\pi+\omega_k)}$, where ω_k is defined as the angle in $[-\frac{\pi}{2}, \frac{\pi}{2}]$ such that $\sin(\omega_k) = \frac{\sin k}{\sqrt{2}}$. The corresponding eigenvectors are displayed in Appendix B. For definiteness, here we consider the time evolution of a particle that begins at the origin in the "left" chirality state. In the Fourier basis this initial state is represented by $\tilde{\Psi}(k,0) = (1,0)^T$ for all k. The wave function at time t is then given by:

$$\tilde{\psi}_{\mathrm{L}}(k,t) = \frac{1}{2}\Big(1 + \frac{\cos k}{\sqrt{1+\cos^2 k}}\Big)\, \mathrm{e}^{-\mathrm{i}\omega_k t} \;+\; \frac{(-1)^t}{2}\Big(1 - \frac{\cos k}{\sqrt{1+\cos^2 k}}\Big)\, \mathrm{e}^{\mathrm{i}\omega_k t} \tag{4}$$

$$\tilde{\psi}_{\mathrm{R}}(k,t) = \frac{\mathrm{i}\mathrm{e}^{\mathrm{i}k}}{2\sqrt{1+\cos^2 k}}\big(\mathrm{e}^{-\mathrm{i}\omega_k t} - (-1)^t \mathrm{e}^{\mathrm{i}\omega_k t}\big) \tag{5}$$

We now invert the Fourier transformation, to return to the basis in real space (cf. Appendix A). The wave functions in real space can be written in the form:

$$\psi_{\mathrm{L}}(n,t) \;=\; \frac{1+(-1)^{n+t}}{2}\int_{-\pi}^{\pi}\frac{dk}{2\pi}\,(1+\frac{\cos k}{\sqrt{1+\cos^2 k}})\,\mathrm{e}^{-\mathrm{i}(\omega_k t+kn)} \tag{6}$$

$$\psi_{\mathrm{R}}(n,t) \;=\; \frac{1+(-1)^{n+t}}{2}\int_{-\pi}^{\pi}\frac{dk}{2\pi}\,\frac{\mathrm{e}^{\mathrm{i}k}}{\sqrt{1+\cos^2 k}}\,\mathrm{e}^{-\mathrm{i}(\omega_k t+kn)} \tag{7}$$

Notice that the amplitudes vanish for even n (respectively, odd n) at odd t (even t), as we would expect from the definition of the walk.

Thus, we have obtained a closed form solution for the time evolved wave function of the Hadamard walk. In view of possible applications to developing Quantum algorithms, we are naturally led to considering the behaviour of the wave functions at large times ($t \gg 1$). Happily, the problem is considerably simplified in this asymptotic limit which allows us to accurately derive several useful results. In the next section, we give details of this asymptotic analysis.

3 Asymptotic properties of the wave function in the large time limit

In the previous section, we obtained an exact solution for the time evolution of the Hadamard walk. In what follows, we will use extensively the Method of Stationary Phase (see Appendix A) to extract the asymptotic properties of the resulting wave function.

3.1 The asymptotic probability distribution

The asymptotic analysis for ψ_{L} and ψ_{R} is essentially the same. They can both be written as a sum of integrals of the type $I(\alpha,t)$ described in Appendix B. Here, α should be understood as n/t. Appendix B gives the details of the analysis for this generic integral; we summarise the conclusions below.

The asymptotics for the wave function are simple to describe. The wave function is essentially uniformly spread over the interval between $\mp 1/\sqrt{2}$ (and so there its gross behaviour is like $1/\sqrt{t}$), and it dies out very fast (faster than any inverse polynomial in t) outside the interval. At the "frontiers" at $\mp 1/\sqrt{2}$, however, there are two peaks of width $O(t^{1/3})$ where the wave function goes as $t^{-1/3}$. The net probability below these two peaks and beyond $\mp 1/\sqrt{2}$ thus goes as $t^{-1/3}$, and does not affect the properties of the wave function we are interested in. We will therefore restrict our attention to the interval $\alpha \in (-1/\sqrt{2}, 1/\sqrt{2})$. The exact expressions for the leading terms of $\Psi = (\psi_{\mathrm{L}}, \psi_{\mathrm{R}})$ for such α are displayed in Appendix B.

We can calculate the probability of observing the particle doing the quantum walk at any given point $n = \alpha t$ from the wave function derived above. Below we give the asymptotic distribution for points $n = \alpha t$ for α between $-1/\sqrt{2}+\epsilon$ and $1/\sqrt{2}-\epsilon$, for an arbitrarily small constant $\epsilon > 0$.

$$P(\alpha,t) \;=\; |\psi_{\mathrm{L}}(\alpha t,t)|^2 + |\psi_{\mathrm{R}}(\alpha t,t)|^2$$

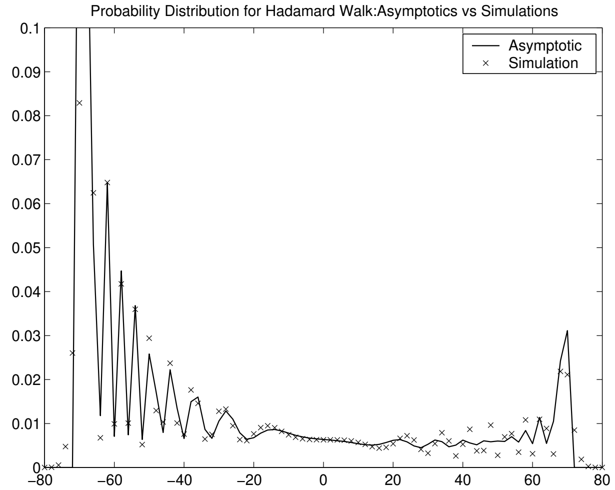

Figure 2: *A comparison of two probability distributions, one obtained from a computer simulation of the Hadamard walk, and the other from from an asymptotic analysis of the walk. The number of steps in the walk was taken to be* 100*. Only the probability at the* even *points is plotted, since the odd points have probability zero.*

$$\sim \quad \frac{1+(-1)^{(\alpha+1)t}}{\pi t\, |\omega''_{k_\alpha}|} \times \\ \Big[(1-\alpha)^2 \cos^2(\phi(\alpha)\, t + \pi/4) \quad + \quad (1-\alpha^2)\cos^2(\phi(\alpha)\, t + k_\alpha + \pi/4)\Big]\,, \tag{8}$$

where $\phi(\alpha) = -\omega_{k_\alpha} - \alpha k_\alpha$, and k_α is the root of $\omega'_k + \alpha = 0$ in $[0, \pi]$.

The (approximate) probability distribution P compares very well with simulation results even for small t, as is evident from Figure 2. The bias to the left in the probability distribution plotted in the figure is an artifact of the choice of initial chirality state (it was chosen to be "left"). If the particle begins in the chirality state $\frac{1}{\sqrt{2}}(|\mathrm{L}\rangle + \mathrm{i}|\mathrm{R}\rangle)$, the distribution at any time turns out to be symmetric (cf. Appendix D, and Figure 5 in the appendix). Indeed, the Hadamard walk is an *unbiased* walk.

3.2 Calculation of the moments

We show in Appendix C that the net probability of the points n with $\alpha = n/t$ between $-1/\sqrt{2} + \epsilon$ and $1/\sqrt{2} - \epsilon$, where ϵ is an arbitrarily small constant, is $1 - \frac{2\epsilon}{\pi} - \frac{O(1)}{t}$, so the rest of the points do not contribute to any global properties of the distribution. Henceforth, we restrict ourselves to this interval.

For the purposes of calculating the moments of the distribution, it will be convenient to decompose P as

$$P(\alpha, t) \quad = \quad P_{\mathrm{slow}}(\alpha, t) + P_{\mathrm{fast}}(\alpha, t), \tag{9}$$

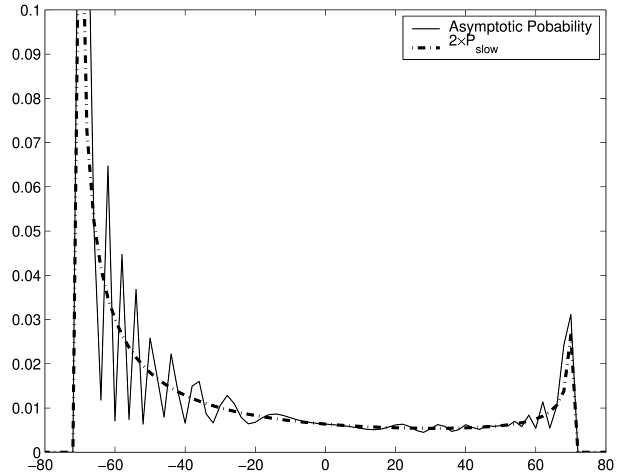

Figure 3: *A comparison of the distributions P and P_{slow} for $t = 100$. Only the probability at the* even *points is plotted, and P_{slow} is scaled by a factor of 2 because it has support on the odd points as well.*

where

$$P_{\text{slow}}(\alpha, t) \quad = \quad \frac{1-\alpha}{\pi t\,|\omega''_{k_\alpha}|} \tag{10}$$

is a slowly varying (non-oscillating) function in α, and P_{fast} is the remaining (quickly oscillating) component. By the analysis shown in Appendix C, we can show that any contribution to a moment from the "fast" component P_{fast} is of lower order in t than the contribution from P_{slow}. In Figure 3, we compare P_{slow} with P.

The calculation of moments is further simplified by the following observation. Let $p(\alpha) = tP_{\text{slow}}(\alpha, t)$. Then p is a probability density function over the interval between $\mp 1/\sqrt{2}$: it is clearly non-negative, and we show below that it integrates to 1. This observation allows us to approximate the sums in the moment calculations by a *Riemann integral*, and the error so introduced is again a lower order term (cf. Appendix C).

To see that $p(\alpha)$ integrates to 1, note that $\frac{\partial\phi}{\partial k}(k_\alpha, \alpha) = 0 = -\omega'_{k_\alpha} - \alpha$, so

$$|\omega''_{k_\alpha}| \quad \equiv \quad -\omega''_{k_\alpha} \quad = \quad \frac{d\alpha}{dk_\alpha}. \tag{11}$$

Now,

$$\int_{-1/\sqrt{2}}^{1/\sqrt{2}} p(\alpha)\,d\alpha \quad = \quad \frac{1}{\pi}\int_{-1/\sqrt{2}}^{1/\sqrt{2}} (1-\alpha)\frac{dk_\alpha}{d\alpha}\,d\alpha \quad = \quad \frac{1}{\pi}\int_0^\pi \left(1 + \frac{\cos k}{\sqrt{1+\cos^2 k}}\right) dk \quad = \quad 1,$$

since the function $\cos k/\sqrt{1+\cos^2 k}$ is anti-symmetric around the point $\pi/2$.

The different moments for the density function p are now readily calculated by standard methods from complex residue theory. Some of these are listed in Figure 4 for comparison with simulation results. This gives us the leading term for the moments for the distribution P.

	$p(\alpha)$	simulation
$\langle\alpha\rangle$	$-1+1/\sqrt{2}=-0.293$	-0.293
$\langle\lvert\alpha\rvert\rangle$	$1/2$	0.500
$\langle\alpha^2\rangle$	$1-1/\sqrt{2}=0.293$	0.293

Figure 4: *A table of moments calculated with the approximation by the density function* $p(\alpha)$*, which are compared with computer simulation results with* $t=80$*. As mentioned before, the particle has a constant speed to the left, as indicated by its mean position, which is a result of its biased initial state. For an unbiased initial state, the mean would be zero.*

3.3 Mixing behaviour of the walk

It is quite evident from Figure 2 that the probability distribution P is almost uniform over the interval between $-1/\sqrt{2}, 1/\sqrt{2}$. We argue this formally below.

Recall that the δ-mixing time (τ_δ) of a random process is defined as the first time t such that the distribution at time t is at total variation distance (which is half the ℓ_1 distance) at most δ from the uniform distribution. We claim that there is a constant $\delta<1$ such that at time t, P is δ-close to the uniform distribution on the integer points between $\mp t/\sqrt{2}$. We emphasise that for classical symmetric random walk, the corresponding mixing time is *quadratic* in t.

In order to show that the Hadamard walk is "mixed" at time t (in the sense described above), it suffices to show that a constant fraction $\beta>0$ of the points in the said interval have probability between $c/\sqrt{2}\,t$ and $1/\sqrt{2}\,t$ for a constant $c>0$. A straightforward calculation shows that this implies that the ℓ_1 distance from uniform over $[-t/\sqrt{2},\ t/\sqrt{2}]$ is at most $2(1-\beta c)$, so that $\delta = 1-\beta c<1$ is a constant.

As in the previous section, we restrict ourselves to the interval where $n/t=\alpha\in[-1/\sqrt{2}+\epsilon,\ 1/\sqrt{2}-\epsilon]$ (with ϵ chosen to be a suitable constant) such that $P(\alpha,t)$ is at most $1/\sqrt{2}t$ within the interval. Recall that the probability mass within this interval is $1-\frac{2\epsilon}{\pi}-\frac{O(1)}{t}$, which is a constant greater than 0 (see Appendix C for a proof of this). Clearly, this cannot hold unless at least a constant fraction $\beta=1-\frac{2\epsilon}{\pi}-c$ of the points within this interval have probability at least some constant $0<c<1-\frac{2\epsilon}{\pi}$ over $\sqrt{2}\,t$. This completes the proof of the mixing nature of the Hadamard walk.

4 Discussion

In this paper, we defined and studied the behaviour of quantum walks on the line, and showed a linear time mixing behaviour for these walks. This has an immediate bearing on the similar walks defined on the circle. It is easy to derive the wave function for the walk on the circle, since it is exactly the wave function for the unbounded line wrapped around the circle. The linear time mixing for the circle is immediate. It is also possible to derive the wave function for an appropriately modified walk on the *finite* line using the solution to the unbounded walk. We expect that this walk be mixing in linear time as well, but leave the details to [16]. (Note that because of boundary effects, the mixing of the walk on a finite line does not follow directly from our results if the walk begins close to the edges.)

Aharonov *et al.* [1] have defined quantum walks on general graphs in the same manner. It would be interesting to characterise the class of graphs on which quantum walks mix faster than classical ones. A promising candidate is the class of Cayley graphs, which seem to be amenable to analysis along the same lines as ours because of their rich group-theoretic structure. It would also be interesting to study how much speed-up is possible in general, and for different classes of graphs. The lower bound result of [1] is a step in this direction.

Our work leads to a plethora of questions regarding the properties of quantum walks. It is yet unclear which of these are interesting from an algorithmic point of view. Any speed-up of a known classical algorithm based on random walk (such as those mentioned in Section 1) seems to involve the analysis of quantum walk on graphs much more complex than the line. However, we believe such analysis is still tractable.

Finally, we ask if it is possible to design quantum algorithms to generate certain desirable superpositions efficiently—those corresponding to distributions that are classically hard to sample from (much in the spirit of [15]). It is conceivable that such algorithms follow an approach that is completely different from the standard Markov chain Monte Carlo method.

Acknowledgements

We would like to thank Mike Saks for discussions on the asymptotic behaviour of integrals and for directing us to [3].

References

[1] Dorit Aharonov, Andris Ambainis, Julia Kempe, and Umesh Vazirani. Personal communication, October 2000.

[2] Andris Ambainis, Eric Bach, and John Watrous. Personal communication, October 2000.

[3] Carl M. Bender and Steven A. Orszag. *Advanced Mathematical Methods for Scientists and Engineers*. International Series in Pure and Applied Mathematics. McGraw-Hill, Inc., New York, 1978.

[4] Norman Bleistein and Richard A. Handelsman. *Asymptotic Expansions of Integrals*. Holt, Rinehart and Winston, New York, 1975.

[5] Persi Diaconis. *Group Representations in Probability and Statistics*, volume 11 of *Lecture Notes-Monograph Series*. Institute of Mathematical Statistics, Hayward, California, 1988.

[6] Martin Dyer, Alan Frieze, and Ravi Kannan. A random polynomial-time algorithm for approximating the volume of convex bodies. *Journal of the ACM*, 38(1):1–17, January 1991.

[7] H. Dym and H. P. McKean. *Fourier Series and Integrals*, volume 14 of *Probability and Mathematical Statistics*. Academic Press, New York, 1972.

[8] Lov K. Grover. A fast quantum mechanical algorithm for database search. In *Proceedings of the Twenty-Eighth Annual ACM Symposium on the Theory of Computing*, pages 212–219, Philadelphia, Pennsylvania, 22–24 May 1996.

[9] Mark Jerrum and Alistair Sinclair. Approximating the permanent. *SIAM Journal on Computing*, 18(6):1149–1178, December 1989.

[10] Mark Jerrum and Alistair Sinclair. The Markov chain Monte Carlo method: An approach to approximate counting and integration. In Dorit S. Hochbaum, editor, *Approximation Algorithms for NP-hard Problems*, chapter 12, pages 482–520. PWS Publishing, Boston, 1996.

[11] Mark Jerrum, Alistair Sinclair, and Eric Vigoda. A polynomial-time approximation algorithm for the permanent of a matrix with non-negative entries. Technical Report TR00-079, Electronic Colloquium on Computational Complexity, http://www.eccc.uni-trier.de/eccc/, 2000.

[12] László Lovász and Ravi Kannan. Faster mixing via average conductance. In *Proceedings of the Thirty-First Annual ACM Symposium on Theory of Computing*, Atlanta, Georgia, 1–4 May 1999. ACM.

[13] David A. Meyer. From quantum cellular automata to quantum lattice gases. *Journal of Statistical Physics*, 85:551–574, 1996.

[14] Rajeev Motwani and Prabhakar Raghavan. *Randomized Algorithms*. Cambridge University Press, 1995.

[15] Ashwin Nayak, Leonard Schulman, and Umesh Vazirani. Unpublished, 1997.

[16] Ashwin Nayak and Ashvin Vishwanath. In preparation, October 2000.

[17] Christos H. Papadimitriou. On selecting a satisfying truth assignment. In *Proceedings of the 32nd Annual Symposium on Foundations of Computer Science*, pages 163–169, San Juan, Puerto Rico, 1–4 October 1991. IEEE Computer Society.

[18] Dana Randall and David Wilson. Sampling spin configurations of an ising system. In *Proceedings of the Tenth Annual ACM-SIAM Symposium on Discrete Algorithms*, pages S959–960, Baltimore, Maryland, 17–19 January 1999.

[19] Uwe Schöning. A probabilistic algorithm for k-SAT and constraint satisfaction problems. In *Proceedings of the 40th Annual Symposium on Foundations of Computer Science*, New York City, NY, 17–19 October 1999. IEEE Computer Society.

[20] Peter W. Shor. Polynomial-time algorithms for prime factorization and discrete logarithms on a quantum computer. *SIAM Journal on Computing*, 26(5):1484–1509, October 1997.

[21] Daniel R. Simon. On the power of quantum computation. *SIAM Journal on Computing*, 26(5):1474–1483, October 1997.

[22] John Watrous. Quantum simulations of classical random walks and undirected graph connectivity. In *Proceedings of the Annual IEEE Conference on Computational Complexity*, pages 180–187, Atlanta, Georgia, USA, 4–6 May 1999.

A Technical background

In this section, we give details of the concepts and results from mathematical analysis that we use in the paper.

A.1 The Fourier transform

Let $f : \mathcal{Z} \rightarrow \mathcal{C}$ be a complex valued function over the integers. Then its Fourier transform $\tilde{f} : [-\pi, \pi] \rightarrow \mathcal{C}$ is defined as

$$\tilde{f}(k) \;=\; \sum_n f(n)\, \mathrm{e}^{\mathrm{i}kn}.$$

The corresponding inverse Fourier transform is then given by

$$f(n) \;=\; \frac{1}{2\pi} \int_{-\pi}^{\pi} \tilde{f}(k)\, \mathrm{e}^{-\mathrm{i}kn}\, dk.$$

Note that this is the dual view of the Fourier transform on the space of functions on $[-\pi, \pi]$.

We will be concerned with functions f with finite support, i.e., functions which are zero except at finitely many points n. The Fourier transforms are extremely well behaved for this class of functions. For more details on the properties of these transforms, see, for example, [7].

A.2 Asymptotic expansion of integrals

Studying the large time behaviour of quantum walks naturally leads us to consider the behaviour of integrals of the form

$$I(t) \;=\; \int_a^b g(k) \mathrm{e}^{\mathrm{i}\, t\, \phi(k)}\, dk \tag{12}$$

as t tends to infinity. There is a well-developed theory of the asymptotic expansion of integrals which allows us to determine, very precisely, the leading terms in the expansion of the integral in terms of simple functions of t (such as inverse powers of t). Below, we explain an important technique known as the Method of Stationary Phase [3, 4] from this theory.

Intuitively, the method may be understood as follows. The exponential in the integral is a rapidly oscillating function if t is large (and if ϕ is not constant in any subinterval). If g is a smooth function of k, then the contributions from adjacent subintervals nearly cancel each other out, and the major contribution to the value of the integral comes from the region where the oscillations are least rapid. The regions of slow oscillation occur precisely at the *stationary points* of the function ϕ, i.e, points c where $\phi'(c) = 0$. (If no such point exists, we can get the asymptotic expansion for I in terms of inverse powers of t by repeated integration by parts, and the integral decays faster than $\frac{1}{t}$.) So the significant terms in the expansion of the integral come from a small interval around the stationary points. The "flatness" of ϕ at a stationary point then determines the contribution of its neighbourhood to the integral. For example, if $\phi''(c) \neq 0$, then the integral goes as $\frac{1}{\sqrt{t}}$, however if $\phi''(c) = 0$ but $\phi'''(c) \neq 0$, then the integral goes as $\frac{1}{t^{1/3}}$.

Without going into the details of its derivation, we state the leading term in the expansion of $I(t)$ assuming that it has exactly one stationary point, and that it occurs at the left end point a of the interval. (Any integral may be written as a sum of such integrals.) We also assume that g is smooth and non-vanishing at a. Suppose a is a stationary point of order $p-1$, i.e., $\phi'(a) = \phi''(a) = \cdots = \phi^{(p-1)}(a) = 0$ but $\phi^{(p)}(a) \neq 0$, then the dominant behaviour of I is given by

$$I(t) \quad \sim \quad g(a)\, \mathrm{e}^{\mathrm{i}t\phi(a) \pm \mathrm{i}\pi/2p} \left[\frac{p!}{t\,|\phi^{(p)}(a)|} \right]^{1/p} \frac{\Gamma(1/p)}{p}, \qquad t \to +\infty, \tag{13}$$

where we use the factor $\mathrm{e}^{\mathrm{i}\pi/2p}$ (respectively, $\mathrm{e}^{-\mathrm{i}\pi/2p}$) if $\phi^{(p)}(a) > 0$ (if $\phi^{(p)}(a) < 0$). For the reader interested in more details about this and other associated techniques, we recommend [3, 4].

B Solution to the Hadamard walk

The following are the two eigenvectors of the matrix M_k for the Hadamard walk mentioned in Section 2.2. (Recall that ω_k is defined as the angle in $[-\frac{\pi}{2}, \frac{\pi}{2}]$ such that $\sin(\omega_k) = \frac{\sin k}{\sqrt{2}}$.)

$$\begin{aligned}
\Phi_k^1 &= \frac{1}{\sqrt{2}} \left((1 + \cos^2 k) - \cos k \sqrt{1 + \cos^2 k} \right)^{-\frac{1}{2}} \begin{bmatrix} \mathrm{e}^{-\mathrm{i}k} \\ \sqrt{2}\,\mathrm{e}^{-\mathrm{i}\omega_k} - \mathrm{e}^{-\mathrm{i}k} \end{bmatrix} \\
\Phi_k^2 &= \frac{1}{\sqrt{2}} \left((1 + \cos^2 k) + \cos k \sqrt{1 + \cos^2 k} \right)^{-\frac{1}{2}} \begin{bmatrix} \mathrm{e}^{-\mathrm{i}k} \\ -\sqrt{2}\,\mathrm{e}^{\mathrm{i}\omega_k} - \mathrm{e}^{-\mathrm{i}k} \end{bmatrix}.
\end{aligned}$$

We now get the expression for the Fourier transform at time t, given the initial state from the identity

$$\tilde{\Psi}(k,t) \quad = \quad \mathrm{e}^{-\mathrm{i}\omega_k t} \, \langle \Phi_k^1 | \tilde{\Psi}(k,0) \rangle \; \Phi_k^1 \quad + \quad \mathrm{e}^{\mathrm{i}(\pi + \omega_k)t} \, \langle \Phi_k^2 | \tilde{\Psi}(k,0) \rangle \; \Phi_k^2.$$

The expressions for $\tilde{\psi}_{\mathrm{L}}, \tilde{\psi}_{\mathrm{R}}$ stated in Section 2.2 are derived by calculating this for a particle that begins the walk at the origin with chirality "left" (i.e., with $\tilde{\Psi}(k,0) = (1,0)^T$ for all k).

We now turn to determining the asymptotic behaviour of the wave function Ψ as t tends to $+\infty$. It suffices to consider an integral of the form

$$I(\alpha, t) \quad = \quad \int_{-\pi}^{\pi} \frac{dk}{2\pi}\, g(k)\, \mathrm{e}^{\mathrm{i}\,\phi(k,\alpha)\,t}, \tag{14}$$

where $g(k)$ is analytic, and a periodic function of period 2π taken to be either even or odd, $\phi(k,\alpha) = -(\omega_k + \alpha k)$, and $\alpha \in [-1,1]$. The integrals in the expressions for $\psi_{\mathrm{L}}, \psi_{\mathrm{R}}$ are exactly of this kind.

It turns out that for large t, the integral $I(\alpha,t)$ has three distinct kinds of behaviour depending on the value of $|\alpha|$, with sharp transitions from one behaviour to the other. It decays faster than any inverse polynomial in t for $|\alpha| > \frac{1}{\sqrt{2}} + O(t^{-2/3})$, goes as $t^{-1/3}$ in an $O(t^{-2/3})$ interval around $\pm\frac{1}{\sqrt{2}}$, and as $t^{-1/2}$ in the remaining interval. Below, we show these behaviours for I for $|\alpha| > \frac{1}{\sqrt{2}} + \epsilon$, $|\alpha| = \frac{1}{\sqrt{2}}$, and $|\alpha| < \frac{1}{\sqrt{2}} - \epsilon$, for any constant $\epsilon > 0$, and leave the more detailed analysis of the transitions from one behaviour to another to [16].

First, we concentrate on $|\alpha|$ larger than $\frac{1}{\sqrt{2}}$ by a constant. For this range of α, ϕ does not have any stationary points, and we can use integration by parts to show the vanishing nature of I.

Before we sketch a proof for this, we calculate some quantities that will also be of use later.

$$\frac{\partial\phi}{\partial k} = -(\omega_k' + \alpha) = -\frac{\cos k}{\sqrt{1+\cos^2 k}} - \alpha \tag{15}$$

$$\frac{\partial^2\phi}{\partial k^2} = -\omega_k'' = \frac{\sin k}{(1+\cos^2 k)^{3/2}} \tag{16}$$

$$\frac{\partial^3\phi}{\partial k^3} = -\omega_k''' = \frac{2\cos k\,(1+\sin^2 k)}{(1+\cos^2 k)^{5/2}} \tag{17}$$

Note that for $|\alpha| \geq 1/\sqrt{2} + \epsilon$, $\left|\frac{\partial\phi}{\partial k}\right| \geq \epsilon$, so its inverse is an analytic function in k. Let

$$u(k) = \frac{g(k)}{\mathrm{i}\,t\,\frac{\partial\phi}{\partial k}}, \qquad \text{and} \qquad v(k) = \mathrm{e}^{\mathrm{i}\phi(k)\,t}.$$

(In the above, we suppress the dependence of the functions on α for ease of notation.) Now, integrating by parts,

$$I(\alpha,t) \equiv \int_{-\pi}^{\pi} \frac{dk}{2\pi}\, u\, \frac{\partial v}{\partial k} = [u(\pi)v(\pi) - u(-\pi)v(-\pi)] - \int_{-\pi}^{\pi} \frac{dk}{2\pi}\, v\, \frac{\partial u}{\partial k}.$$

The first term above is 0 because of periodicity, and the integrand in the second term is bounded (in magnitude) by c_ϵ/t for some constant c_ϵ that depends only on ϵ. To prove a similar statement for any greater power of t, we may use induction with the invariant that the integral resulting from the previous integration by parts is of the same form as I.

We now look at the points $\alpha = 1/\sqrt{2}, -1/\sqrt{2}$. At these points, ϕ has a stationary point of order 2 at $k = \pi, 0$, respectively, as may readily be verified. Using the method of stationary phase, we thus get the following leading term for I at these points:

$$I(\frac{1}{\sqrt{2}},t) \sim \frac{g(\pi)}{3\pi}\sqrt{2}\,\Gamma(1/3)\left[\frac{6}{t}\right]^{1/3}\cos\left(\frac{\pi}{\sqrt{2}}t + \frac{\pi}{6}\right)$$

$$I(-\frac{1}{\sqrt{2}},t) \sim \frac{g(0)}{6\pi}\sqrt{\frac{3}{2}}\,\Gamma(1/3)\left[\frac{6}{t}\right]^{1/3}.$$

Finally, we turn to the interval of most interest to us, $[-1/\sqrt{2}+\epsilon, 1/\sqrt{2}-\epsilon]$. When α lies in this region, ϕ has two stationary points $k_\alpha, -k_\alpha$, where $k_\alpha \in [0,\pi]$ and

$$\cos k_\alpha = \frac{-\alpha}{\sqrt{1-\alpha^2}}. \tag{18}$$

The phase and its second derivative at the stationary points are:

$$\begin{aligned} \phi(\pm k_\alpha, \alpha) &= \mp(\omega_{k_\alpha} + \alpha k_\alpha) && (19) \\ \frac{\partial^2 \phi}{\partial k^2}(\pm k_\alpha, \alpha) &= \mp \omega_k'' = \pm(1-\alpha^2)\sqrt{1-2\alpha^2}. && (20) \end{aligned}$$

We abbreviate $\phi(k_\alpha, \alpha)$ by $\phi(\alpha)$. We can again employ the method of stationary phase to get the dominant term in the expansion for I:

$$I(\alpha, t) \sim \frac{g(k_\alpha)}{\sqrt{2\pi t\,|\omega_{k_\alpha}''|}} \times \begin{cases} 2\cos(\phi(\alpha)\,t + \pi/4) & \text{if } g \text{ is even} \\ 2\mathrm{i}\sin(\phi(\alpha)\,t + \pi/4) & \text{if } g \text{ is odd} \end{cases} \tag{21}$$

Using the above analysis, we can write out the asymptotic expressions for $\psi_{\mathrm{L}}, \psi_{\mathrm{R}}$:

$$\left.\begin{array}{l} \psi_{\mathrm{L}}(\alpha t, t) \\ \\ \psi_{\mathrm{R}}(\alpha t, t) \end{array}\right\} \sim \frac{1+(-1)^{(\alpha+1)t}}{\sqrt{2\pi t\,|\omega_{k_\alpha}''|}} \times \left\{\begin{array}{l} (1-\alpha)\cos(\phi(\alpha)\,t + \pi/4) \\ \\ \alpha\,\cos(\phi(\alpha)\,t+\pi/4) \\ -\sqrt{1-2\alpha^2}\,\sin(\phi(\alpha)\,t+\pi/4) \end{array}\right. \tag{22}$$

It is now straightforward to calculate the probability distribution $P(\alpha, t)$ induced on the line by observing the position of the particle after t steps of the walk. Equation 8 in Section 3 gives the asymptotic expression for $P(\alpha, t)$.

Our estimate of the probability distribution is compared with computer simulations in Figure 2 of Section 3. In Figure 5, we give a plot of the distribution obtained with the symmetric initial chirality state $\frac{1}{\sqrt{2}}(|\mathrm{L}\rangle + \mathrm{i}|\mathrm{R}\rangle)$. The figure illustrates the unbiased nature of the Hadamard walk. We leave the details of the calculation of the asymptotic behaviour of the distribution to [16].

C Justification for approximations made in section 3

In calculating the moments of the probability distribution $P(\alpha, t)$ obtained by observing a particle doing the Hadamard walk, we made two approximations. First, we decomposed P into a slowly varying, non-oscillating part P_{slow} and a quickly oscillating part P_{fast}. We claimed that the contribution to the moments from P_{fast} is of smaller order in t. Then, we approximated the moment sums involving P_{slow} by a Reimann integral. In this section, we will sketch proofs that the error involved in the two approximations both go as $1/t$ times the quantity being estimated.

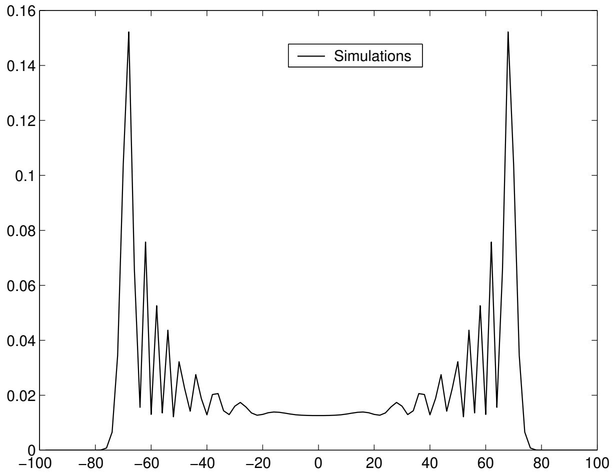

Figure 5: *The probability distribution obtained from a computer simulation of the Hadamard walk with a symmetric initial condition. The number of steps in the walk was taken to be* 100*. Only the probability at the* even *points is plotted, since the odd points have probability zero.*

As an important consequence of the error bound we derive, we show that the net probability of points in the range $\alpha \in [-1/\sqrt{2}+\epsilon,\ 1/\sqrt{2}-\epsilon]$ differs from the integral of the density function

$$p(\alpha) \quad = \quad \frac{1-\alpha}{\pi\,|\omega''_{k_\alpha}|} \tag{23}$$

over this interval by $O(1)/t$. This integral equals $1 - \frac{2\epsilon}{\pi}$.

In the following discussion, we assume that $n/t, \alpha \in [-1/\sqrt{2}+\epsilon,\ 1/\sqrt{2}-\epsilon]$ (this range also applies to sums over n, integrals over α etc.).

First, we bound the error in approximating a moment sum using P_{slow} by an integral. We compute the moments in terms of fractions of the appropriate powers of t. For the mth moment ($m \geq 0$),

$$\begin{aligned}\left|\sum_n (n/t)^m P_{\text{slow}}(n/t,t) - \int_\alpha \alpha^m p(\alpha,t)\,d\alpha\right| \quad &\leq \quad \sum_n \int_{n/t}^{(n+1)/t} d\alpha\ \left|(n/t)^m t\, P_{\text{slow}}(n/t,t) - \alpha^m p(\alpha)\right| \\ &\leq \quad \sum_n \int_{n/t}^{(n+1)/t} d\alpha\,\Delta_{1/t}(\alpha^m p(\alpha)) \end{aligned} \tag{24}$$

where

$$\Delta_\delta f(\alpha) \quad = \quad \max_\alpha |f(\alpha+\delta) - f(\alpha)|\,.$$

It is easy to verify that the variation given by $\Delta_{1/t}$ for $\alpha^m p(\alpha)$ over α in the interval above is $O(1)/t$. This gives an error bound of $O(1)/t$ in equation (24) above.

We now show a bound of $O(1)/t$ on the error introduced by the first kind of approximation mentioned above, namely by ignoring P_{fast}, the component of P with quickly oscillating factors. We bound one of the terms occurring in it; the others may be bounded similarly. Consider the following term obtained from equation (8) in Section 3, by expressing the sine and cosine functions in terms of exponentials:

$$\tilde{P}(\alpha, t) \quad = \quad \frac{\alpha(1-2\alpha)}{\pi t |\omega''_{k_\alpha}|} \mathrm{e}^{2\mathrm{i}\phi(\alpha)\, t},$$

where $\phi(\alpha) \stackrel{\text{def}}{=} \phi(k_\alpha, \alpha)$. We estimate it's contribution to the mth moment. The basic observation is that each term in the moment sum such as $\alpha^m \tilde{P}(\alpha, t)$ is essentially the leading term in the asymptotic expansion of an integral of the type in equation (12) discussed Appendix A:

$$\alpha^m \tilde{P}(\alpha, t) \quad \sim \quad \frac{1}{\sqrt{t}} \int_\delta^{\pi-\delta} dk\, f(k)\, \mathrm{e}^{2\mathrm{i}\phi(k,\alpha)\, t},$$

where

$$f(k) \quad = \quad -2(\omega'_k)^{m+1}(1+2\omega'_k) \frac{\mathrm{e}^{-\mathrm{i}\pi/4}}{\pi\sqrt{\pi|\omega''_k|}},$$

and δ is a suitable constant. The expression for f above is derived using the identity $\alpha = -\omega'_{k_\alpha}$ and comparing the term in the moment sum with the asymptotic form of the integral in equation (13) in Appendix A. The error introduced by this integral representation is $O(t^{-3/2})$.

We may now bound the contribution to the moment sum due to $\tilde{P}$ as

$$\begin{aligned} \sum_n (n/t)^m \tilde{P}(\alpha, t) \quad &\sim \quad \frac{1}{\sqrt{t}} \sum_n \int_\delta^{\pi-\delta} dk\, f(k)\, \mathrm{e}^{-2\mathrm{i}\omega_k t - 2\mathrm{i}nk} \\ &= \quad \frac{1}{\sqrt{t}} \int_\delta^{\pi-\delta} dk\, f(k)\, \mathrm{e}^{-2\mathrm{i}\omega_k t} \sum_n \mathrm{e}^{-2\mathrm{i}nk} \\ &= \quad \frac{1}{\sqrt{t}} \int_\delta^{\pi-\delta} dk\, f(k)\, \mathrm{e}^{-2\mathrm{i}\omega_k t}\, \frac{\mathrm{e}^{-2\mathrm{i}k(\beta t+1)} - \mathrm{e}^{2\mathrm{i}k\beta t}}{\mathrm{e}^{-2\mathrm{i}k} - 1}, \end{aligned}$$

where $\beta = (1/\sqrt{2} - \epsilon)$. We may now use the method of stationary phase again to derive the asymptotic form of the integral. As we expect from the analysis we did in Appendix B, the integral goes as $1/\sqrt{t}$, and thus the entire expression goes as $1/t$.

D General walk on the line

So far we have been describing the details of the Hadamard walk on the line. Here, we consider the properties of the general quantum walk on the line. As mentioned in Section 1, it suffices to consider a particle that carries a "left" or "right" chirality, and at each time step undergoes a unitary transformation of its chirality state and then moves accordingly, one step to the right if it ends in "right" chirality state, and one step to the left if it ends in the "left" chirality state. The most general such unitary transformation contains four parameters. However, it can be shown [16] that if we focus on the probability distribution that results from these walks, then there is a *single* parameter that labels a family of walks, and every element of the family gives rise to identical probability distributions $P(n,t)$ for the same initial conditions. The walks given by this parameter are also singled out for study in [13].

We therefore consider a representative element from each family, which we write as

$$\begin{aligned} M(\theta) &= T \circ (I \otimes U_\theta), \qquad \text{where} && (25)\\ T &= T_- \otimes |\mathrm{L}\rangle\langle\mathrm{L}| + T_+ \otimes |\mathrm{R}\rangle\langle\mathrm{R}|, \qquad \text{and} && (26)\\ U_\theta &= \mathrm{e}^{\mathrm{i}\,\frac{\theta}{2}\,\sigma_y}. && (27) \end{aligned}$$

The operator $M(\theta)$ evolves the state by one time step, i.e., $|\Psi(t+1)\rangle = M(\theta)|\Psi(t)\rangle$, the operator T implements the left/right shift ($T_+|n\rangle = |n+1\rangle$ while $T_-|n\rangle = |n-1\rangle$), and U_θ is the unitary transformation acting on the chirality state. The Hadamard walk belongs to the family of walks parametrised by $\theta = \frac{\pi}{2}$. To show this we write the Hadamard transform as

$$H = \frac{1}{\sqrt{2}} \begin{pmatrix} 1 & 1 \\ 1 & -1 \end{pmatrix} = -\mathrm{i}\,\mathrm{e}^{\mathrm{i}\,\frac{\pi}{2}\,\sigma_z}\,\mathrm{e}^{\mathrm{i}\,\frac{\pi}{4}\,\sigma_y} = -\mathrm{i}\,\mathrm{e}^{\mathrm{i}\,\frac{\pi}{2}\,\sigma_z}\,U_{\frac{\pi}{2}}. \qquad (28)$$

Thus, by a suitable redefinition of phase of the chirality states at time $t+1$, the additional rotation that multiplies $U_{\frac{\pi}{2}}$ can be absorbed. Clearly, the probability distributions for finding a particle at a point are unaffected by this redefinition of phase. Therefore, the Hadamard walk is equivalent to the walk with $\theta = \frac{\pi}{2}$.

The behaviour of the walk with $\theta = 0$ and $\theta = \pi$ are easily analysed. When $\theta = 0$, the unitary transformation rotating the chirality states is the identity, and hence a particle starting with "left" ("right") chirality, after t time steps, moves t units to the left (right). This walk is clearly not mixing, since the probability is concentrated at one or two points at any given instant, and resembles more the biased classical walk (though we wish to emphasise here that all the quantum walks we consider are *unbiased*, a point which we return to below). Now, when $\theta = \pi$, the unitary transformation flips the chirality at each time step. Hence a particle zig-zags between the origin and a neighbouring point, and thus has a non-zero probability on a maximum of three points. This walk too is clearly not mixing.

For intermediate values of θ the behaviour is more involved, as our analysis of the Hadamard walk indicates. In fact, the qualitative behaviour of the Hadamard walk is generic to all θ excluding the singular values $0, \pi$ that we discussed above. All of these walks are mixing, and mix in linear time.

We can calculate very easily some properties of the general walk, following the analysis for the Hadamard walk. We first note that the eigenvalues of $M_k(\theta)$ for the general walk given by θ are

$$\begin{aligned} \lambda_k^1(\theta), \lambda_k^2(\theta) &= \mathrm{e}^{\pm\mathrm{i}\,\omega_k(\theta)}, \qquad \text{where} && (29)\\ \cos(\omega_k(\theta)) &= \cos\frac{\theta}{2}\cos k && (30) \end{aligned}$$

where $\omega_k(\theta) \in [0, \pi]$.

It is possible to deduce the relevant component P_{slow} of the asymptotic probability distribution P from the eigenvalues in equation (29), as is evident from the case of the Hadamard walk. The distribution P_{slow} beginning with symmetric initial conditions is:

$$P_{\text{slow}}(\alpha, t) \;=\; \frac{1}{\pi t\, \omega''_{k_\alpha}(\theta)} \tag{31}$$

and has support on the interval $\alpha \in (-\cos\frac{\theta}{2},\ \cos\frac{\theta}{2})$. Here k_α is given by the usual stationary point condition:

$$\left.\frac{d\omega_k(\theta)}{dk}\right|_{k=k_\alpha} \;=\; \alpha, \tag{32}$$

and the derivatives of $\omega_k(\theta)$ with respect to k are

$$\omega'_k(\theta) \;=\; \frac{\sin k \cos\frac{\theta}{2}}{\sin(\omega_k(\theta))} \tag{33}$$

$$\omega''_k(\theta) \;=\; \cot(\omega_k(\theta))\,[1 - (\omega'_k(\theta))^2]. \tag{34}$$

Thus the stationary points are $k_\alpha, \pi - k_\alpha$, where $k_\alpha \in [-\pi/2,\ \pi/2]$ and

$$\sin k_\alpha \;=\; \frac{\alpha}{\sqrt{1-\alpha^2}}\tan\frac{\theta}{2}. \tag{35}$$

The second derivative of the phase at the stationary points is $\pm\omega''_{k_\alpha}(\theta)$ where

$$\omega''_{k_\alpha}(\theta) \;=\; \frac{1-\alpha^2}{\sin\frac{\theta}{2}}\sqrt{\cos^2\frac{\theta}{2} - \alpha^2}. \tag{36}$$

We can readily verify that the probability sums to one, i.e.,

$$t\int d\alpha\, P_{\text{slow}}(\alpha, t) \;=\; \int d\alpha\, \frac{1}{\pi\, \omega''_{k_\alpha}(\theta)} \;=\; \int_{-\pi/2}^{\pi/2} \frac{dk_\alpha}{\pi} \;=\; 1, \tag{37}$$

where we have used the fact that $\omega''_{k_\alpha} = \frac{d\alpha}{dk_\alpha}$. Thus, as in the case of the Hadamard walk, almost all the probability is confined to the interval between $\mp\cos\frac{\theta}{2}$ and is close to uniform over it.

In order to compare the mixing characteristics of the walks with different θ, we may compare the distribution after t time steps for each of these with a fixed distribution, say the uniform distribution over the interval $[-t, t]$. Notice that the "height" of the distribution with parameter θ is proportional to $\sin\frac{\theta}{2}$, so the distance from uniform increases to 1 as $\theta \to 0$. Similarly, as $\theta \to \pi$, the "width" of the distribution (which is proportional to $2\cos\frac{\theta}{2}$) goes to zero, and the distance from uniform tends to 1. Figure 6 plots the distribution P_{slow} for different values of θ.

The distribution P_{slow} can, as before, be used to calculate moments. For example, the mean position of the particle $\langle|\alpha|\rangle$ is given by

$$\int d\alpha\, |\alpha|\, t P_{\text{slow}}(\alpha, t) \;=\; 2\int_0^{\frac{\pi}{2}} \frac{dk_\alpha}{\pi}\, \omega'_{k_\alpha}(\theta) \;=\; 1 - \frac{\theta}{\pi}, \tag{38}$$

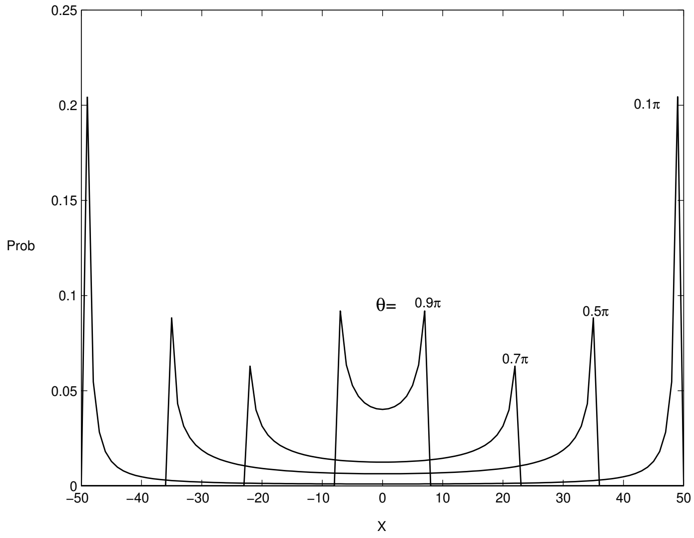

Figure 6: *A comparison of probability distributions* P_{slow} *for different values of* θ *(with symmetric initial conditions). The number of time steps* t *was taken to be* 50 *here.*

which matches the expected value at the points $\theta = 0, \frac{\pi}{2}, \pi$.

Finally we comment on the unbiased nature of the quantum walks defined in this manner. An unbiased walk (starting at the origin) does not distinguish between the left and right halves of the line, i.e., it is reflection symmetric. In order to capture this into a condition on unbiased walks, it is necessary to also account for the initial chirality state of the particle which can lead to a biased probability distribution, although the rules governing the walk are intrinsically reflection symmetric. Therefore, although such a symmetric walk can produce a biased probability distribution with some particular initial condition, there exists another initial condition for which the bias is exactly reversed. In more formal terms, if we describe the quantum walk by the matrices M_k in equation (1) in Section 2, then we need to find a unitary matrix S such that:

$$S^\dagger M_k S = M_{-k}. \tag{39}$$

The unitary matrix S performs a rotation on the chirality state that reverses any bias arising from the choice of initial condition. If no such matrix exists, then the walk intrinsically distinguishes left from right and is hence not an unbiased walk[4]. An immediate consequence is that if we start with an initial chirality state that is an eigenvector of S, then a symmetric probability distribution is generated. For the family of walks just considered, the unitary matrix $S = \sigma_y$ will suffice since it only interchanges T_+ and T_- and does nothing else. Therefore, starting in the initial chirality state $\frac{1}{\sqrt{2}}(|\mathrm{L}\rangle \pm \mathrm{i}|\mathrm{R}\rangle)$ generates a symmetric distribution, as shown for the Hadamard walk in Figure 5.

[4] Actually the condition is a little more general, an overall sign change can also be permitted, i.e., $S^\dagger M_k S = \pm M_{-k}$. In fact, the minus sign appears for the Hadamard walk, where $S = \sigma_y$.